UDC 621.315.592

## Experimental and analytical study of the mechanical stress compensation problem in the InGaAs multiple quantum wells for near-infrared light emitting diodes

© R.A. Salii<sup>1,2</sup>, A.V. Malevskaya<sup>1</sup>, D.A. Malevskii<sup>1</sup>, S.A. Mintairov<sup>1</sup>, A.M. Nadtochiy<sup>2</sup>, N.A. Kalyuzhnyy<sup>1</sup>

<sup>1</sup> loffe Institute.

194021 St. Petersburg, Russia

<sup>2</sup> Alferov University,

194021 St. Petersburg, Russia

E-mail: r.saliy@mail.ioffe.ru Received April 28, 2025 Revised July 19, 2025 Accepted July 27, 2025

The applicability of various methods for calculating the optimal thickness of compensating layers for InGaAs multiple quantum wells used in the active area of (Al)GaAs near-infrared light emitting diodes grown on vicinal substrates with different angle of misorientation is considered. High accuracy of the considered methods for structures, grown on substrates with small misorientation angle (up to  $2^{\circ}$ ) is experimentally demonstrated. For structures on strongly misoriented substrates ( $6^{\circ}+$ ), the applicability of the methods is limited to finding the thickness of compensating layers in the first approximation. Light emitting diodes with high efficiency ( $62^{\circ}$ %), quantum efficiency ( $57^{\circ}$ %) and high optical power at a current of up to 1 A are created.

Keywords:quantum well, LED, InGaAs, MOVPE, heterostructures.

DOI: 10.61011/SC.2025.04.61713.7907

Quantum well (QW) structures are widely used in semiconductor devices such as near-infrared (IR) laser diodes [1], fiber-optical amplifiers and light-emitting diodes (LED) [2]. In addition to LED wavelength and light energy spectrum control, QWs provide improved internal quantum efficiency of a device [1,2], and multiple QWs (MQW) [3] provide high optical power output. However, there are two restrictions for a thermodynamically stable MQW layer system that are induced, first, by a critical thickness limit of an individual stressed (lattice mismatched with the matrix) QW and, second, by the fact that each MQW will increase the total stress of the whole array leading to relaxation in upper layers [4]. By compensating the compressive strain of one stressed layer induced by another "tensile" layer (or vice versa), the critical thickness of the QW array may be increased significantly [5] without defect formation in the LED's active area. A wide set of computational models is described in the literature to find the best properties of compensating layers (CL) [6]. They include both evaluation models and more precise models based, in particular, on classical elasticity theory [7,8]. Such models are reasonably applicable to structures grown on exactly oriented wafers. In thin film growth processes on the vicinal surfaces of wafers, due consideration shall be given to potential influence of kinetic barriers, and applicability of precise models to the MQW growth on wafers with strongly misoriented surfaces is not proved.

This study investigates InGaAs/AlGaAs heterostructures (HS) containing MQWs that were used to form an active

area of IR LED emitting at 940 nm. These devices are widely used in medical diagnosis, optical communications, night vision systems, etc. [9]. Their HSs are grown by metallorganic vapor-phase epitaxy (MOVPE) and, thus, on vicinal wafers. The objective of the study was to check experimentally the applicability of both evaluation and more precise models for calculating CL properties for MQW structures grown using the MOVPE technique on wafers with various degrees of surface misorientation (100).

Compensation of compressive and tensile strain induced by stressed and compensating layers shall achieve conditions where the stress in the growth plane between each MQW period will be minimized. To evaluate the average stress  $(\varepsilon_a)$  induced by one MQW period, it is convenient to use the following expression [10]

$$\varepsilon_a = \frac{t_1 \varepsilon_1 + t_2 \varepsilon_2}{t_1 + t_2},\tag{1}$$

where  $t_i$  are stressed and compensating layer thicknesses,  $\varepsilon_i$  is the stress induced by a corresponding layer with respect to the wafer that is calculated as

$$\varepsilon_i = \frac{a_0 - a_i}{a_i},\tag{2}$$

where  $a_0$  and  $a_i$  are the wafer and layer lattice constants, respectively.

The MOVPE technique was used to grow HS containing MQW with CL and emitting at 940 nm at room temperature. Models described below were used to calculate the

 Layer
 a, Å
  $C_{11}$ , dyne/cm²
  $C_{12}$ , dyne/cm²
 A, dyne/cm²

 In<sub>0.14</sub>Ga<sub>0.86</sub>As (QW)
 5.710
  $1.140 \cdot 10^{12}$   $5.228 \cdot 10^{11}$   $1.184 \cdot 10^{12}$  

 GaAs<sub>0.92</sub>P<sub>0.08</sub> (CL)
 5.637  $1.207 \cdot 10^{12}$   $5.409 \cdot 10^{11}$   $1.263 \cdot 10^{12}$ 

Table 1. Crystallographic parameters of MQW layers

Table 2. Calculated CL parameters for four models

Method No	Abbreviation	Expression for t <sub>2</sub>	$t_2,  ext{Å}$	$\varepsilon_a, \text{mln}^{-1} \text{ (ppm)}$
1	ALM	(4)	249	28
2	TWM	(6)	246	0
3	TWM+A	(8)	230	-146
4	ZSM	(10)	227	-176

optimum CL thickness  $(t_2)$ . Lattice constants of the matrix, stressed QW layer and CL  $(a_0, a_1 \text{ and } a_2, \text{ respectively})$ , and the stressed QW layer thickness  $(t_1)$  were used as fixed values for the calculations.

1) An average lattice method (ALM) — is a simplified method where stress-balanced condition occurs in the structure when the lattice constants of compressive and tensile layers are averaged over thickness. The condition implies an expression for the matrix lattice constant derived from the work of Matthews and Blakeslee [11] with an approximation that the compressive and tensile layers have identical stiffness parameters:  $a_0 = (t_1a_1 + t_2a_2)/(t_1 + t_2)$ . Thus, the expression for the desired CL thickness is written as:

$$t_2 = \frac{t_1(a_0 - a_1)}{a_2 - a_0}. (3)$$

2) The thickness weighted strain method (TWM) suggests that a strain-balanced structure emerges from equivalent strain thickness products for the tensile and compressive layers:

$$t_1\varepsilon_1 + t_2\varepsilon_2 = 0. (4)$$

By substituting (2) into (4), an expression for the corresponding matrix lattice constant  $(a_0)$  may be written, from which an expression or thickness  $t_2$  may be derived:

$$t_2 = -\frac{a_2 t_1 (a_0 - a_1)}{a_1 (a_0 - a_2)}. (5)$$

3) This model may be refined by taking into account a difference in stiffness parameters for stressed and compensating layer materials (TWM+A method):

$$A_1t_1\varepsilon_1 + A_2t_2\varepsilon_2 = 0, (6)$$

where  $A_i$  are the stiffness parameters depending on the stiffness coefficients  $C_{i1}$  and  $C_{i2}$  as follows:  $A_i = C_{i1} + C_{i2} - 2C_{i2}^2/C_{i1}$ . In this case, by substituting (2) into (7), we get the following expression for the wafer lattice constant and, consequently, for the CL thickness:

$$t_2 = -\frac{a_2 A_1 t_1 (a_0 - a_1)}{a_1 A_2 (a_0 - a_2)}. (7)$$

4) A zero stress method (ZSM) proposed in [6] using classical elasticity theory [7] offers the following zero mean stress in the growth surface plane:  $A_1t_1\varepsilon_1a_2 + A_2t_2\varepsilon_2a_1 = 0$ . From this, CL lattice constants and CL thickness may be calculated:

$$t_2 = t_1 \left[ \frac{A_1 a_2^2 (a_0 - a_1)}{A_2 a_1^2 (a_2 - a_0)} \right]. \tag{8}$$

Calculation using the above-mentioned models was performed for pairs of InGaAs QW and GaAsP CL layers composing one MQW period in the test InGaAs/AlGaAs HS grown on GaAs wafers by the MOVPE technique. Al<sub>0.3</sub>Ga<sub>0.7</sub>As, a wide-band material, that didn't absorb IR light and included the active area consisting of five In<sub>0.14</sub>Ga<sub>0.86</sub>As QWs with GaAs<sub>0.92</sub>P<sub>0.08</sub> CL served as the basis for HS. Composition and thickness (70 Å) of the In<sub>0.14</sub>Ga<sub>0.86</sub>As QW layers were calculated to form the 940 nm radiation [12]. HSs were grown on two types of GaAs (100) wafers: "weakly misoriented" wafers, i.e. at 2° in the (110) direction (such HSs are hereinafter referred to as W2), and MOVPE-typical wafers — misoriented at 6° in the (111) direction (hereinafter referred to as W6).

Crystallographic parameters for the InGaAs layers were calculated using [13], and determined for  $GaAs_{0.92}P_{0.08}$  using Vegard's law (see Table 1). The optimum thicknesses of  $GaAs_{0.92}P_{0.08}$  CL calculated for all four models and for the corresponding mean stress using equation (1) are listed in Table 2.

 $\varepsilon_a$ , that is equal to zero from the TWM calculation, follows from the stress balance condition for this method (expression (4)). The calculated data predicts the optimum thickness of GaAs<sub>0.92</sub>P<sub>0.08</sub> CL in the range from 23 to 25 nm. According to the simplified model (ALM), it shall be equal to  $\sim 25$  nm, while the most precise ZSM, that includes mechanical parameters of both layers, predicts the optimum thickness of  $\sim 23$  nm. Therefore, the CL thickness varied in a range close to the calculated one, i.e. within 20–27 nm, during the growth of the above-mentioned HSs. In addition, for comparative analysis enhancement, HSs were grown on both types of vicinal wafers, CL thicknesses of which deviated greatly from the calculated properties

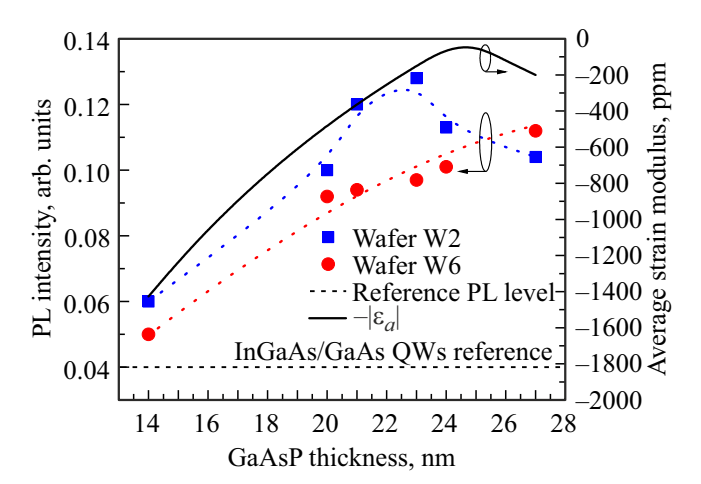


**Figure 1.** Dependence of the PL intensity maximum measured at room temperature on the GaAs<sub>0.92</sub>P<sub>0.08</sub> CL thickness for InGaAs/AlGaAs heterostructures grown on vicinal wafers W2 (squares) and W6 (circles). PL intensity level for the reference sample without CL is shown dashed, the solid line shows the calculated dependence of  $\varepsilon_a$  (Expression (1)).

and were equal to 14 nm. A reference structure with five  $In_{0.14}Ga_{0.86}As$  MQWs free of any CLs, that used GaAs as intermediate layers, was also grown. Despite the fact that the well thickness is smaller than the critical thickness of the  $In_{0.14}Ga_{0.86}As$  layer in the GaAs matrix, at which, according to the Matthews— Blakeslee model, mismatch dislocation is generated and which is  $\sim 10\,\mathrm{nm}$ , the mean stress in the reference structure is still very high,  $|\varepsilon_a| = 2326\,\mathrm{mln}^{-1}$ .

Experimental HSs with MQW were studied by examining the photoluminescence (PL) spectra excited by the DTL-413 solid-state laser with  $\lambda = 527$  nm. Figure 1 shows the dependence of PL peak intensities measured at room temperature on the GaAs<sub>0.92</sub>P<sub>0.08</sub> CL thickness for both types of vicinal wafers.

Note first that the measurements for HS with CL are more than twice as high as those for the reference sample without CL in terms of the PL intensity maximum (the reference level is shown dashed in Figure 1) suggesting that a mechanical stress technique is necessary for formation of high quality MQW. However, CL with quite arbitrarily chosen parameters (in this case with  $t_2 = 14 \, \mathrm{nm}$ ) very slightly improves the radiative capability of structures.

On the contrary, for all structures with CL thicknesses close to the design range, the PL intensity was much better and at sufficiently close level. Nevertheless, for structures W2 (Figure 1, squares), a clear maximum on the dependence of the PL intensity on the GaAs<sub>0.92</sub>P<sub>0.08</sub> CL thickness may be reported. This maximum correlates well with the ZSM and refined TWM (CL thickness is  $\sim 23\,\text{Å}$ ) calculation data, and with calculated values of  $\varepsilon_a$  (Figure 1, solid line). Thus, the described models may be certainly applicable to the thickness evaluation of CL grown both on exactly oriented and slightly misoriented wafers. However, methods taking into account the stiffness parameters A of MQW layers (such as TWM+A and ZSM) provide the most precise evaluation of the optimum CL thickness.

For W6 HS (Figure 1, circles), i.e. MOVPE-typical strongly misoriented wafers, the experimental result is not so unambiguous. PL intensity continued growing slightly as  $t_2$  varied from 20 to 27 nm. However, note that of all methods, the ALM calculation is the simplest one, that doesn't require tabular data on material stiffness coefficients and predicts the largest CL thickness. A conclusion may be made that ALM turns out to be sufficient to get the first-approximation CL thickness in HS grown on strongly misoriented wafers. Then the optimum CL thickness may be refined experimentally as, for example, in [14]. A more complex method to calculate the optimum CL thickness in HS on wafers with misorientation > 2° may include the above-mentioned methods where strain and stress are addressed as second-rank tensors with corresponding C (fourth-rank tensors) [8]. However, taking into account

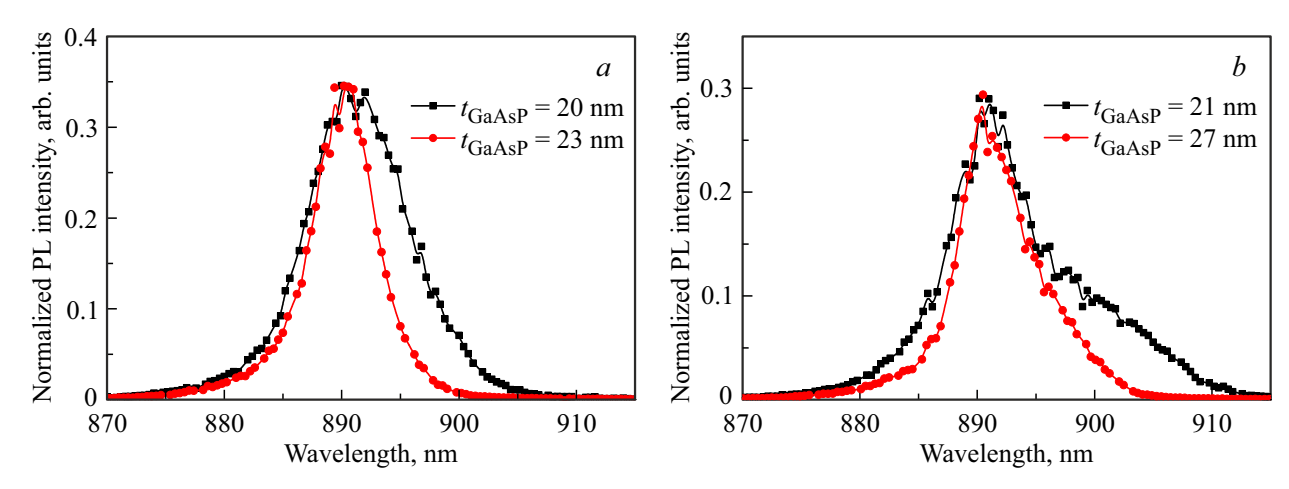


**Figure 2.** Normalized PL spectra for the InGaAs/AlGaAs heterostructures measured at low temperature (77 K) for samples with different CL thickness grown on wafers W2 (a) and W6 (b).

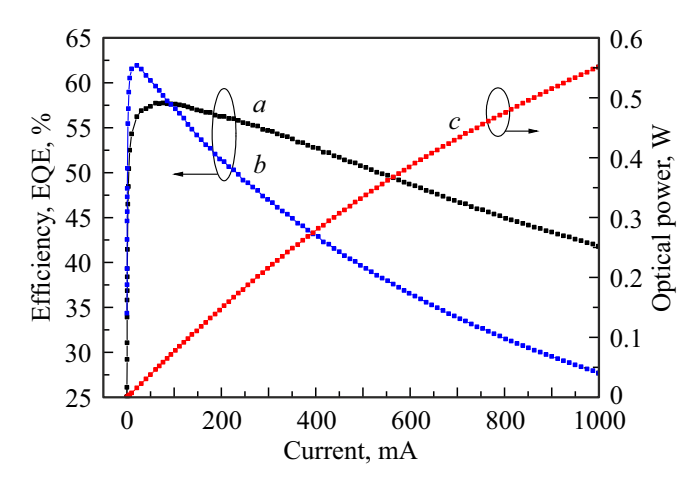


**Figure 3.** Dependences of the efficiency (a), external quantum efficiency (b) and optical power (c) of LED based on InGaAs MQW containing optimized GaAsP CL.

that the simplest method is already able to evaluate the parameters for HS demonstrating the maximum PL, this calculation may be only of academic interest.

Comparison of PL spectra measured at 77 K confirms additionally that the found values of  $t_2$  for both heterostructures are close to optimum values. For convenience, these PL spectra are normalized by intensity (Figure 2). In both cases, HSs with near-optimum CL thickness (23 nm for W2 and 27 nm for W6) are compared with HSs, CL thickness of which is at the boundary of the given calculation range (20–21 nm). PL spectra from HS with "boundary" CL thicknesses have long-wavelength broadening of the spectrum and general increase in FWHM of the PL peak.

The studied MQW structures with optimized CL were used in the active area of LED heterostructures with 940 nm. LEDs fabricated using the developed post-growth techniques [15,16] demonstrated high optical power (> 77 mW at  $100 \, \text{mA}$ ) and high external quantum efficiency (57%) and efficiency  $\sim 62 \, \%$  (Figure 3). Due to defect-free QW stacking, LED performance is demonstrated at a pumping current up to  $1 \, \text{A}$  with high power output (> 550 mW).

## **Acknowledgments**

The authors appreciate the financial support provided by the Ministry of Science and Higher Education of the Russian Federation (topic FFUG-2025-0005). A.M. Nadtochiy is grateful to the Ministry of Science and Higher Education of the Russian Federation (project FSRM-2023-0010).

## Conflict of interest

The authors declare no conflict of interest.

## References

- [1] L.J. Mawst, H. Kim, G. Smith, W. Sun, N. Tansu. Progr. Quant. Electron., 75, 100303 (2021).DOI: 10.1016/j.pquantelec.2020.100303
- [2] P.D. Nguyen, M. Kim, Y. Kim, J. Jeon, S. Park, C.S. Kim, Q.L. Nguyen, B.S. Chun, S.J. Lee. Heliyon, 10 (3), e25269 (2024). DOI: 10.1016/j.heliyon.2024.e25269
- [3] W.-C. An, H.-G. Kim, L.-K. Kwac, J.-S. So, H.-J. Lee. J. Nanosci. Nanotechnol., 19, 2224 (2019). DOI: 10.1166/jnn.2019.15974
- [4] S. Tundo, M. Mazzer, L. Lazzarini, L. Nasi, G. Torsello,
   D. Diso, G. Clarke, C. Rohr, P. Abbott, K. Barnham,
   R. Ginige. Mater. Sci. Technol., 19 (7), 977 (2003).
   DOI: 10.1179/026708303225004341
- [5] C.W. Tu, X.B. Mei, C.H. Yan, W.G. Bi. Mater. Sci. Eng. B, 35 (1-3), 166 (1995). DOI: 10.1016/0921-5107(95)01434-9
- [6] N.J. Ekins-Daukes, K. Kawaguchi, J. Zhang. Cryst. Growth Des., 2 (4), 287 (2002). DOI: 10.1021/cg025502y
- [7] C. Kittel. *Introduction to Solid State Physics*. 7th edn (John Wiley & Sons, Inc., N.Y., 1996).
- [8] J.F. Nye. Physical Properties of Crystals: Their Representation by Tensors and Matrices (Oxford University Press, N.Y., 1985).
- [9] M. Vasilopoulou, A. Fakharuddin, F. Pelayo García de Arquer, D.G. Georgiadou, H. Kim, Abd. Rashid bin Mohd Yusoff, F. Gao, M.K. Nazeeruddin., H.J. Bolink., E.H. Sargent. Nature Photonics, 15, 656 (2021). DOI: 10.1038/s41566-021-00855-2
- [10] Y. Wang, R. Onitsuka, M. Deura, W. Yu, M. Sugiyama, Y. Nakano. J. Cryst. Growth, 312 (8), 1364 (2010). DOI: 10.1016/j.jcrysgro.2009.11.063
- [11] J.W. Matthews, A.E. Blakeslee. J. Cryst. Growth, **32**, 265 (1976). DOI: 10.1016/0022-0248(76)90041-5
- [12] R.A. Salii, A.V. Malevskaya, D.A. Malevskii, S.A. Mintairov,
   A.M. Nadtochiy, N.A. Kalyuzhnyy. Opt. Spectrosc., 132 (11),
   1146 (2024). (in Russian).
   DOI: 10.61011/OS.2024.11.59501.6568-24
- [13] http://www.matprop.ru
- [14] R.A. Salii, A.V. Malevskaya, D.A. Malevskii, S.A. Mintairov, A.M. Nadtochiy, N.A. Kalyuzhnyy. Kristallografiya 4, 743 (2024). (in Russian). DOI: 10.31857/S0023476124040214
- [15] A.V. Malevskaya, N.D. Ilyinskaya, N.A. Kalyuzhnyy, D.A. Malevskii, Yu.M. Zadiranov, P.V. Pokrovsky, A.A. Blokhin, A.V. Andreeva. FTP, 55 (11), 1086 (2021). (in Russian). DOI: 10.21883/FTP.2021.11.51565.9679
- [16] A.V. Malevskaya, N.A. Kalyuzhnyy, R.A. Salii, F.Yu. Soldatenkov, M.V. Nakhimovich, D.A. Malevskii. Tech. Phys.Lett., 50 (18), 22 (2024). (in Russian).
  DOI: 10.61011/PJTF.2024.18.58625.19946

Translated by E.Ilinskaya